Applied Catalysis B: Environmental 192 (2016) 268–276

Contents lists available at ScienceDirect

Applied Catalysis B: Environmental

journal homepage: www.elsevier.com/locate/apcatb

Enhanced immobilization of ReO_4^- by nanoscale zerovalent iron supported on layered double hydroxide via an advanced XAFS approach: Implications for TcO_4^- sequestration

Guodong Sheng[a,b,*], Yanna Tang[a], Wensheng Linghu[a], Lijun Wang[a], Jiaxing Li[d], Hui Li[a], Xiangke Wang[a,b], Yuying Huang[c]

[a] College of Chemistry and Chemical Engineering, College of Medical Science, Shaoxing University, Zhejiang 312000, PR China
[b] School of Chemistry and Environment, North China Electric Power University, Beijing 102206, PR China
[c] Shanghai Synchrotron Radiation Facility (SSRF), Shanghai Institute of Applied Physics, Chinese Academy of Sciences, Shanghai 201204, PR China
[d] Institute of Plasma Physics, Chinese Academy of Sciences, P.O. Box 1126, Hefei 230031, PR China

ARTICLE INFO

Article history:
Received 6 February 2016
Received in revised form 19 March 2016
Accepted 1 April 2016
Available online 1 April 2016

Keywords:
Layered double hydroxide
Nanoscale zero valent iron
Enhanced immobilization
Re(VII)
Support effect

ABSTRACT

This paper was concentrated on a promising remediation strategy for the reductive immobilization of Tc(VII) by studying its chemical analogue Re(VII) to ease the experimental conditions. A novel composite namely nanoscale zero-valent iron supported on layered double hydroxide (NZVI/LDH) was synthesized and applied for the reductive immobilization of Re(VII). Compared to bare NZVI, the as-synthesized NZVI/LDH exhibited higher efficiency on Re(VII) immobilization due to the good synergistic effect between adsorption and reduction. The precise role of LDH was revealed in detail using an advanced approach. The phrase and morphology analysis indicates that NZVI was uniformly supported on LDH, which apparently reduces the aggregation of NZVI and increases its reactivity. ^{57}Fe Mössbauer spectra suggest that NZVI/LDH displayed a good anti-oxidation performance, leading to the enhanced stability during reaction. X-ray absorption fine structure (XAFS) results show that LDH could promote complete reduction of Re(VII) into Re(IV) by NZVI, while sorption and reduction occurred simultaneously on bare NZVI. Moreover, LDH not only acts as a pH buffering agents but also as a scavenger for the coexisting anions and sparingly soluble products, which improves the reactivity of NZVI. The excellent immobilization performance of NZVI/LDH provides a promising strategy for decontamination of Tc(VII) from groundwater.

1. Introduction

Recently, with the rapid development of nuclear energy, as well as the past cold war era, more and more radionuclides are increasingly discharged into the natural environment, resulting in the widespread contamination of groundwater [1–10]. Technetium-99 (^{99}Tc) is one of the most important fission products of uranium-238 (^{238}U), and its half life is $\sim 2.13 \times 10^5$ years [1–5]. Under oxic conditions, ^{99}Tc is commonly present in the anionic form of pertechnetate (TcO_4^- or Tc(VII)) with high solubility and mobility. Besides, Tc(VII) can be reduced into the sparingly soluble form of Tc(IV) (i.e., $TcO_2 \cdot nH_2O$) under anoxic conditions [1–3,10–12]. Therefore, reductive immobilization of Tc(VII) into Tc(IV) has been regarded as a potentially effective approach for the remediation of Tc-contaminated groundwater.

In the last two decades, zero-valent iron (ZVI) technology have been widely studied for contaminant sequestration in the remediation of soil and groundwater which is contaminated by nitroaromatic compound, chlorinated organic compounds as well as toxic metals due to their suitable redox potentials [13–20]. In comparison with commercial iron powder or granular iron, nanoscale zerovalent iron (NZVI) has recently received much more attention for the in-situ remediation of groundwater due to its large specific surface area, high reactivity as well as strong reduction capacity [21–27]. While NZVI technology holds the promise in environmental pollution clean-up, nevertheless, NZVI tends to aggregate rapidly due to the high surface energy and magnetic force, resulting in the formation of large aggregates, thereby losing its reactivity, durability and efficiency, which greatly hinders the

* Corresponding author at: College of Chemistry and Chemical Engineering, Shaoxing University, Zhejiang 312000, PR China.
E-mail addresses: gdsheng@usx.edu.cn, gdsheng@mail.ustc.edu.cn (G. Sheng).

http://dx.doi.org/10.1016/j.apcatb.2016.04.001
0926-3373/

practical application of NZVI [28–30]. For preventing the aggregation of NZVI and enhancing the speed and efficiency of remediation, particle stabilization has been proposed in many studies by attaching stabilizing agents onto NZVI. These stabilizations are achieved via enhancing the electrostatic repulsions between NZVI particles to inhibit their aggregation and thus increase their stability and reactivity [31–35]. Recently, as an alternative to stabilization approach, supported NZVI has been lately proposed to mitigate the commonly observed aggregation phenomenon [36,37]. Concerning this respective, the commonly used supports include diatomite [38], kaolinite [39], rectorite [40], Na-bentonite [41], raw and modified smectite clay [42–44], Mg-aminoclay [45–47], silica [48], $Mg(OH)_2$ [49], carbon nanotubes [50,51] and graphene oxides [52–55]. These results suggest that implementing suitable support may enhance the dispersive of NZVI in water and thus the supported NZVI represent an effective approach for the in-situ remediation of groundwater. Nevertheless, the precise role of these supports in NZVI has not been clearly verified, particularly using advanced approaches at a molecular level.

Layered double hydroxide (LDH) is a class of anionic clay, and has potential application in the removal of contaminants in water because of their high surface area and strong adsorption capability [56–58]. Besides, LDH can participate in various modifications due to the presence of a great amount of surface hydroxyl groups on LDH. Therefore, a large number of LDH-based multifunctional materials have been synthesized and utilized for the removal of contaminants in environmental pollution control [59–62]. In addition, the adsorption of contaminants onto LDH can promotes the mass transfer of contaminants from solution to iron surface, facilitating the reduction rate [41,62]. Unfortunately, to our knowledge, quite few studies have been reported on utilizing LDH as a support of NZVI for the enhanced immobilization of contaminants. Besides, investigations into variation in the reactivity of supported NZVI when reacted with various groundwater solutes like anions or organic matters have been not actively pursued, despite the importance of the potential roles of coexisting solutes in the reactivity and stability of NZVI, which aids in extending the practical application of supported NZVI in environmental remediation.

The aim of this work was to synthesize a novel composite, i.e., LDH-supported NZVI, and test its effectiveness for the reductive immobilization of $^{99}TcO_4^-$. To ease the work, perrhenate (ReO_4^- or Re(VII)) was used as a chemical analogue of $^{99}TcO_4^-$ due to their similar physical and chemical properties. ReO_4^- has been commonly utilized as a surrogate for $^{99}TcO_4^-$ due to the availability and non-radioactive nature [10,11,63]. The specific goals of this paper were to: (1) synthesize and characterize the composite of LDH-supported NZVI; (2) compare the performance on the immobilization of Re(VII) by bare and supported NZVI; (3) determine the effects of various parameters such as pH and coexisting anions on reduction efficiency; (4) reveal the precise role of LDH in NZVI system using advanced approaches.

2. Experimental approaches

2.1. Materials and chemicals

All the chemicals (like $FeSO_4{\cdot}7H_2O$, $KReO_4$, ReO_2, Na_2SO_4, NaCl, $NaHCO_3$, Na_3PO_4, $NaBH_4$, NaOH, HCl, 1,10-phenanthroline (1,10-phen)) including commercial zero valent iron (ZVI) were purchased from Shanghai Chemical Co., China. The fraction of commercial iron passing through a sieve of 0.15 mm was selected for experiments. All the solutions were prepared with 18 $M\Omega\,cm^{-1}$ high-purity water from a Millipore Milli-Q water purification system. According to our previous work [51,57,62], the layered double hydroxide (LDH) was synthesized by a co-precipitation method, the nanoscale zerovalent iron (NZVI) was synthesized by a $NaBH_4$ reduction approach, the LDH-supported NZVI composite (NZVI/LDH) was synthesized by a similar approach except that LDH was soaking in $FeSO_4{\cdot}7H_2O$ before the launch of $NaBH_4$ reduction. The details are displayed in the Supporting information (SI).

2.2. Macroscopic and characterization approaches

All the macroscopic batch experiments for Re(VII) immobilization onto the reactive materials (LDH, ZVI, NZVI and NZVI/LDH) were carried out at room temperature in a 150-mL glass conical flask undergoing shaking at 100 rpm. The reactive materials and stock solutions of coexisting solutes and Re(VII) were added to obtain the desired concentrations of different components. The reaction system was adjusted to the desired pH by adding negligible volumes of NaOH or HCl with a concentration of 0.01 mol/L. In order to maintain anoxic conditions of the reaction systems, before adding the iron samples, the conical flask with 100 mL of Re(VII) solution was deoxygenated by N_2 stream for 30 min, then, the conical flask was sealed with a stopper during the reaction experiment. To collect enough products for solid characterization, the experiments of Re(VII) immobilization were performed in a 1000-mL conical flask. After reaction, the solid products were filtered and washed, finally vacuum-dried. The collected solid samples were stored in N_2 conditions. The solid samples were characterized by X-ray diffraction (XRD), transmission electron microscope (TEM), scanning electron microscopy images and energy dispersive spectrometer (SEM-EDS), ^{57}Fe Mössbauer spectroscopy (MBS) and X-ray absorption fine structure (XAFS). The Mössbauer spectra were measured at 290 K using a Bench MB-500 Mössbauer spectrometer and an X-ray source of 0.925 GBq $^{57}Co/Rh$. The measured spectra were fitted to Lorentzian line shapes using standard line shape fitting routines. The half-width and peak intensities of the quadruple doublet were constrained to be equal. Isomer shifts were expressed with respect to the centroid of the spectrum of metallic iron foil ($^{56}Fe > 99.85\%$). The X-ray absorption fine structure (XAFS) spectra for the reacted samples of Re(VII) immobilization onto LDH, NZVI, NZVI/LDH and the reference samples (Re(VII) and Re(IV)) were collected on beamline 14W1 at Shanghai Synchrotron Radiation Facility (SSRF, China). The detailed procedures are shown in the SI.

3. Results and discussion

3.1. Characterization results

The surface morphology and elemental composition of the as-synthesized samples were studied by SEM-EDS and TEM. The SEM image of NZVI and NZVI/LDH and corresponding SEM-EDX elemental mapping are displayed in Fig. 1 and Fig. 2, respectively. From the energy spectrum analysis, we can see that the NZVI sample was mainly composed of O(K), Fe(L), while O(K), Fe(L), Al(K), Mg(K) were all present in the NZVI/LDH sample. This result indicates that NZVI were successfully supported on LDH. From the TEM images, we can see that LDH are smooth and well shaped (Fig. S1A). Besides, similar to previous reports, NZVI are spherical with size in the range of 10–100 nm and tend to aggregate together (Fig. S1B), due to van der Waals' force and magnetic properties of the particles. Nevertheless, the typical morphology (Fig. S1C) of NZVI/LDH reveals that NZVI particles were uniformly supported on LDH surface without clear aggregation [49,62]. In lots of previous reports about NZVI supported on cationic layered clay minerals [39–44], generally speaking, the authors indicated that NZVI nanoparticles are clearly discrete and well dispersed on the surface of layered clay without obvious aggregation. In this paper, anionic layered

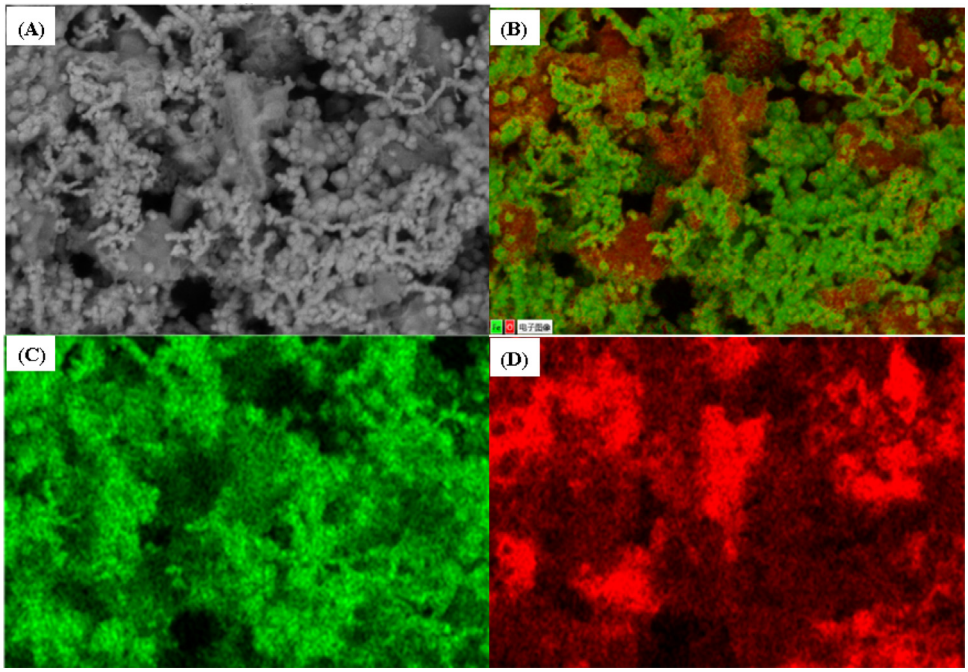

Fig. 1. (A) SEM image of NZVI particle, (B) SEM-EDX elemental mapping image of O(K), Fe(L) on this area, (C) SEM-EDX elemental mapping image of O(K) on this area, (D) SEM-EDX elemental mapping image of Fe(L) on this area.

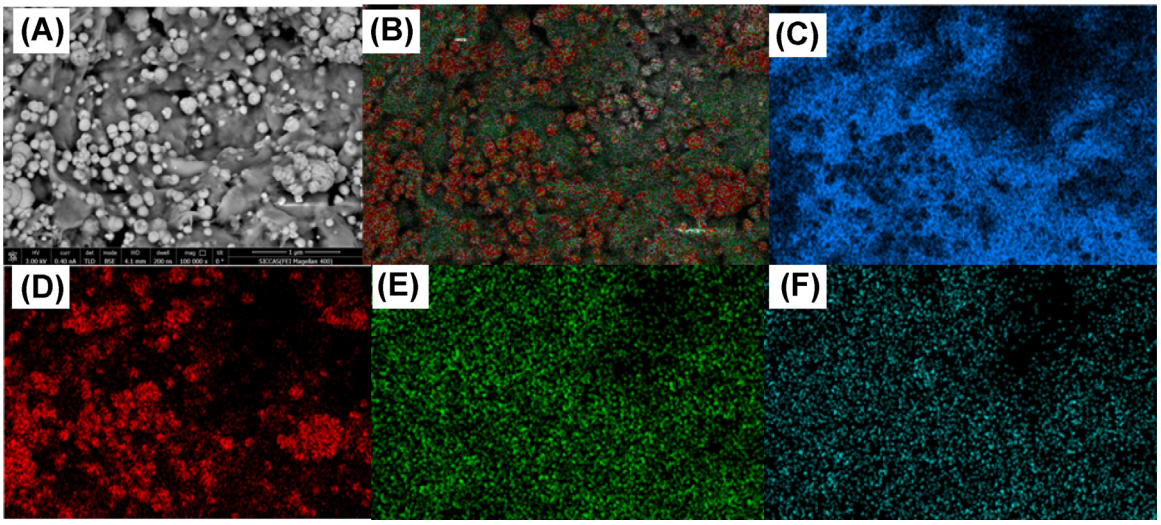

Fig. 2. (A) SEM image of NZVI/LDH particle, (B) SEM-EDX elemental mapping image of O(K), Fe(L), Al(K), Mg(K) on this area, (C) SEM-EDX elemental mapping image of O(K) on this area, (D) SEM-EDX elemental mapping image of Fe(L) on this area, (E) SEM-EDX elemental mapping image of Al(K) on this area, (F) SEM-EDX elemental mapping image of Mg(K) on this area.

clay, i.e., LDH was used to support NZVI. Since there are a large number of surface hydroxyl groups onto LDH, which contributes to the strong complexation of Fe^{2+}, the surface adsorbed Fe^{2+} was reduced into Fe° by $NaBH_4$. So, we think that most of NZVI was deposited on the surface of LDH. Namely, supporting of NZVI on LDH is another effective approach to prevent NZVI from aggregation, which is in good consistency with previous reports [38–55]. The N_2 adsorption-desorption isotherms of the LDH, ZVI, NZVI and NZVI/LDH samples are displayed in Fig. S2. The N_2-BET surface areas measured from the isotherms were 52.4 m^2/g for LDH, 7.51 m^2/g for ZVI, 47.4 m^2/g for NZVI and 42.2 m^2/g for NZVI/LDH, respectively. The XRD patterns of LDH, NZVI and NZVI/LDH are displayed in Fig. S3. For NZVI, the characteristic reflection at ~45.2° is indicative of a pure cubic α-Fe° crystalline structure. For NZVI/LDH, the characteristic peaks at (003), (006), (002) and (113) were ascribed to LDH, and the diffraction peak at (110) was ascribed to α-Fe° phrase, suggesting the good combination of LDH and NZVI. Besides, using atomic absorption spectroscopy (AA-6300C, Shimadzu), the iron contents of the reactive materials were determined to be 90.4% for ZVI, 78.8% for NZVI and 25.8% for NZVI/LDH, respectively.

3.2. Enhanced immobilization of Re(VII) by LDH-supported NZVI

The efficiency of LDH, ZVI, NZVI and NZVI/LDH to immobilize Re(VII) from an aqueous solution with an initial concentration of 150 mg/L at pH ~ 6.5 is shown in Fig. 3A. We can see that ~10.3% of Re(VII) was immobilized onto LDH after 100 min contact which is governed via a sorption process. Meanwhile, ~20.1% of Re(VII)

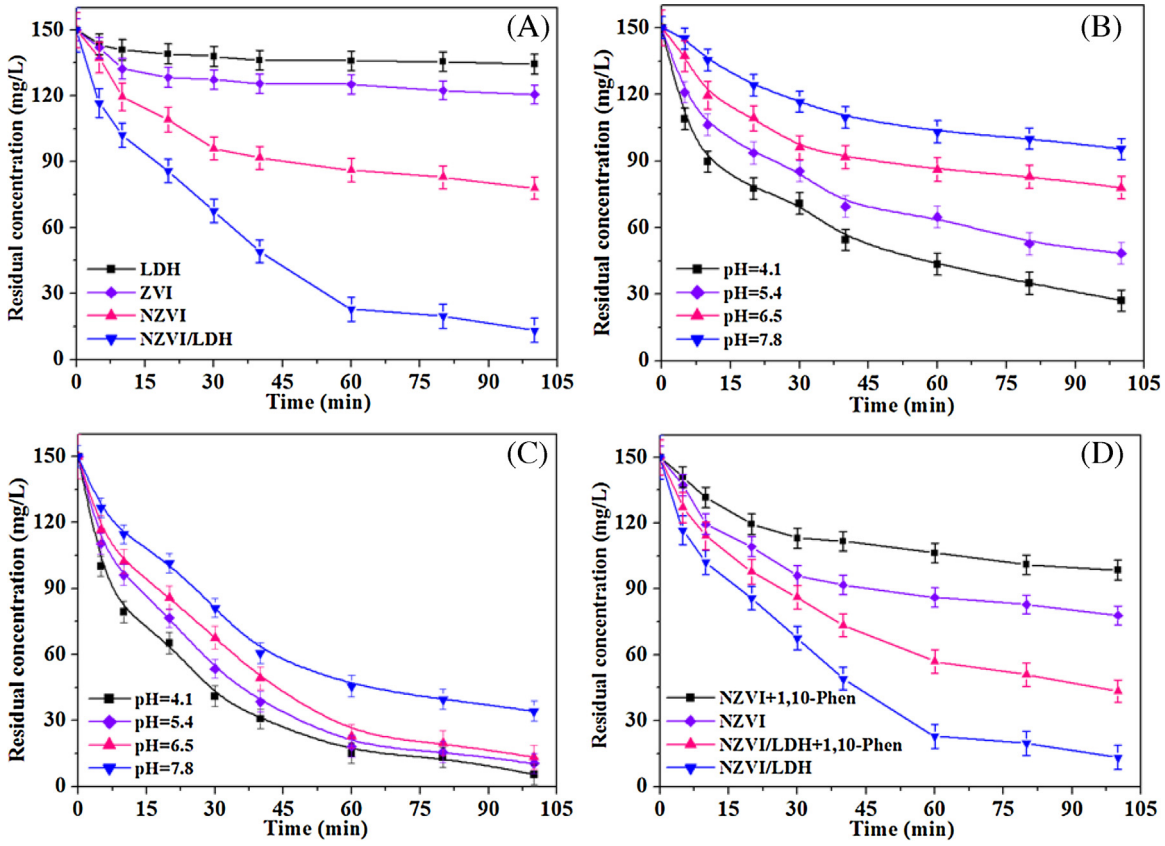

Fig. 3. The comparison of the efficiency for Re(VII) immobilization onto various reactive materials (A), the role of pH in Re(VII) immobilization onto NZVI (B) or NZVI/LDH particle (C), and the role of 1,10-phenanthroline in Re(VII) immobilization onto NZVI or NZVI/LDH particle (D).

was immobilized onto ZVI after 100 min contact, whereas ~48.1% of Re(VII) was immobilized onto NZVI by a reduction process. This phenomenon is in good agreement with previous reports in which NZVI with larger surface area is more reactive than commercial ZVI [64–68]. More importantly, we can find from Fig. 1A that Re(VII) immobilization onto NZVI/LDH (~91.4%) is superior to the sum of NZVI reduction and LDH sorption, displaying that the use of LDH to support NZVI may impose good synergistic effect during Re(VII) immobilization onto NZVI/LDH. The synergistic effect of LDH is to some extent resulted from the sorption of Re(VII) on LDH. Generally speaking, Re(VII) immobilization on NZVI occurs on iron surface, so enrichment of Re(VII) at the interface plays an important role in the surface-mediated reaction [41,67,68]. The sorption isotherm of Re(VII) on LDH was shown in Fig. S4, and we can see that LDH showed good sorption capacity of Re(VII) which is due to the surface electrical property. The zeta potential of LDH as a function of pH was determined in our previous report, and it was clear that the values of zeta potential of LDH were positive at pH < 11.8, which is indicative of a positively-charged surface [62]. Thereby, the positively-charged LDH facilitates the uptake of anionic Re(VII) by attractive interaction, In another word, Re(VII) ions can be well enriched at the solid/water interfaces, and can more easily contact the reactive sites of NZVI, which leads to the acceleration of surface reaction for Re(VII) with iron.

The role of medium pH in Re(VII) immobilization onto NZVI and NZVI/LDH are shown in Fig. 3B and C, respectively. The efficiency of Re(VII) immobilization onto NZVI decreased from 81.9% to 36.7% after 100 min contact, with pH increasing from 4.1 to 7.8, suggesting that Re(VII) immobilization onto NZVI is strongly pH-dependent. It was proposed that Re(VII) was immobilized on NZVI through a redox process (Eqs.(1) and (2)) in which Fe° donates electrons to reduce Re(VII) to Re(IV), and Fe° can be easily oxidized into Fe^{2+} or Fe^{3+} [11].

$$3Fe^{\circ} + 2ReO_4^- + 8H^+ \rightarrow 3Fe^{2+} + 2ReO_2 + 4H_2O \quad (1)$$

$$3Fe^{2+} + ReO_4^- + 4H^+ \rightarrow 3Fe^{3+} + ReO_2 + 2H_2O \quad (2)$$

Therefore, a lower pH favored Re(VII) immobilization due to the accelerated corrosion of NZVI and the decreases of insoluble reaction products on iron surface. Namely, under acidic condition, proton (H^+) can scavenge the passive layer on iron surface to maintain its reactivity. Whereas, iron oxides/hydroxide precipitates can be easily formed under basic condition, and these precipitates on NZVI surface form a passivation layer, inhibiting the contact of Re(VII) with reductive surface. Hence, the efficiency of Re(VII) immobilization decreases at elevated pH.

Nevertheless, we can find from Fig. 3C that the efficiency of Re(VII) immobilization onto NZVI/LDH only decreased from 96.4% to 77.2% when pH increased from 4.1 to 7.8, displaying that the pH role in the reactivity was less pronounced in the case of NZVI/LDH. This phenomenon is in good consistency with previous reports [51,62,67,68], which can be attributed to the buffering effect of surface hydroxyl groups onto LDH. According to Eq. (1), the H^+ ions were strongly needed for Re(VII) reduction by NZVI, thereby, the medium pH gradually increased with H^+ ions being consumed during Re(VII) immobilization [11]. The main role of surface hydroxyl groups on LDH is their ability to produce H^+ ions that can be released into solution and maintain medium pH to a relative low value, subsequently reducing the surface passivation of NZVI [69,70]. The changes of pH values in both NZVI and NZVI/LDH system during Re(VII) immobilization in various processes were determined and shown in Fig. S5. The pH values in both NZVI and NZVI/LDH systems quickly increased within 10 min, after which the pH values

maintained relatively constant. Besides, the final pH values in NZVI system were higher than those in NZVI/LDH system due to the pH buffering effect of LDH. Previously, a combination of iron with various minerals exhibited similar pH buffering behaviors [67–70].

The role of Fe(II) chelating agents (herein, 1,10-phenanthroline) at medium pH = 6.5 in Re(VII) immobilization onto NZVI and NZVI/LDH are shown in Fig. 3D. It is interesting to find that Re(VII) immobilization onto both NZVI and NZVI/LDH was apparently inhibited in the presence of 1,10-phenanthroline, which is ascribed to the formation of a stable complex for 1,10-phenanthroline with Fe(II) produced in-situ, reducing the redox reaction between Fe(II) and Re(VII) according to Eq. (2) [25]. This result reveals that Re(VII) immobilization onto bare or supported NZVI was to some extent attributed to the reduction of Re(VII) by the surface bound Fe(II) besides the reduction of Re(VII) adsorbed on the iron oxides/hydroxides shell by the electrons transferred from the iron core. The indispensable role of these surface bound Fe(II) that contributes to the reduction of contaminants has been widely confirmed by several groups in recent years [11,12,68]. For examples, Liang et al. [15–17] found that the surface adsorbed Fe(II) onto ZVI and/or freshly formed iron oxides/hydroxides could effectively reduce Se(IV)/Se(VI) into Se(0)/Se(-II) in ZVI system. Besides, Mu et al. [71] found that the electrons from both iron core and surface bound Fe(II) on iron oxides/hydroxides shell could lead to Cr(VI) reduction by a Fe@Fe_2O_3 nanowire. Moreover, it was indicated that Fe(II) adsorbed on surfaces in heterogenous reaction systems could effectively reduce U(VI) to U(IV) [41,72]. In previous reports, it was documented that Tc(VII) reduction by dissolved Fe(II) does not occur thermodynamically. However, Fe(II) adsorbed on solid surfaces is proved to show more powerful reduction capacity than dissolved Fe(II) [73,74]. Herein, due to the similar chemistry between Tc(VII) and Re(VII), the same mechanism may be used for Re(VII) reduction, which is the ultimate target radionuclide [73,74]. In another word, in NZVI system, besides NZVI, Fe(II) adsorbed the freshly formed iron oxides/hydroxides also contributes to Re(VII) reduction. In addition, the role of 1,10-phenanthroline in Re(VII) immobilization in NZVI/LDH system is more pronounced than that in NZVI system, indicating that the Fe(II) adsorbed onto LDH is also able to reduce Re(VII) into Re(IV).

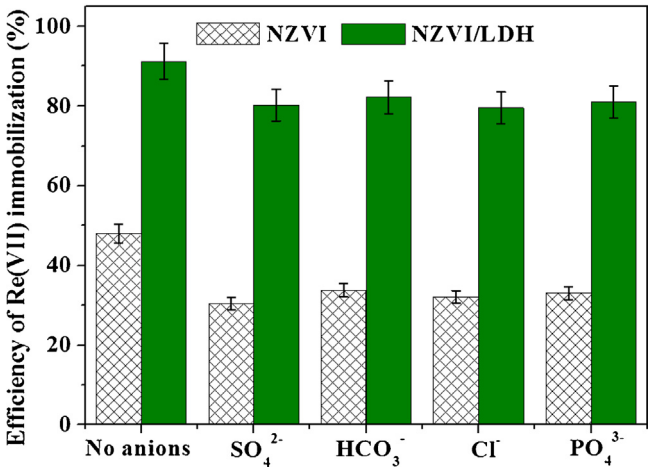

Fig. 4. The role of coexisting anions (i.e., SO_4^{2-}, HCO_3^-, Cl^- and PO_4^{3-}) in Re(VII) immobilization onto NZVI or NZVI/LDH particle.

Fig. 4 illustrates the role of coexisting anions (i.e., SO_4^{2-}, HCO_3^-, Cl^- and PO_4^{3-}) in the reactivity of both NZVI and NZVI/LDH. It is obvious that the presence of these coexisting anions generally triggered a decline of the reactivity of NZVI and NZVI/LDH. This negative role of coexisting anions with respect to the reactivity of various forms of iron is in good consistency with previous studies, in which the tested anions decreased the reactivity of various iron [24,75]. Earlier studies on the roles of coexisting anions in NZVI reactivity reported a trade-off effect between the formation of iron oxides/hydroxides precipitates containing these anions to block the reactive sites on iron surface under high concentration (decreasing reactivity) and the acceleration of iron oxides/hydroxides dissolution on iron under low concentration (increasing reactivity) [75–77]. The high anion concentrations in the present study likely favored the former process, i.e., the formation of iron oxides/hydroxides precipitates on NZVI, which led to the observed decrease in the reactivity. Further, it is notable to observe that the extent of decrease is largely greater in NZVI sys-

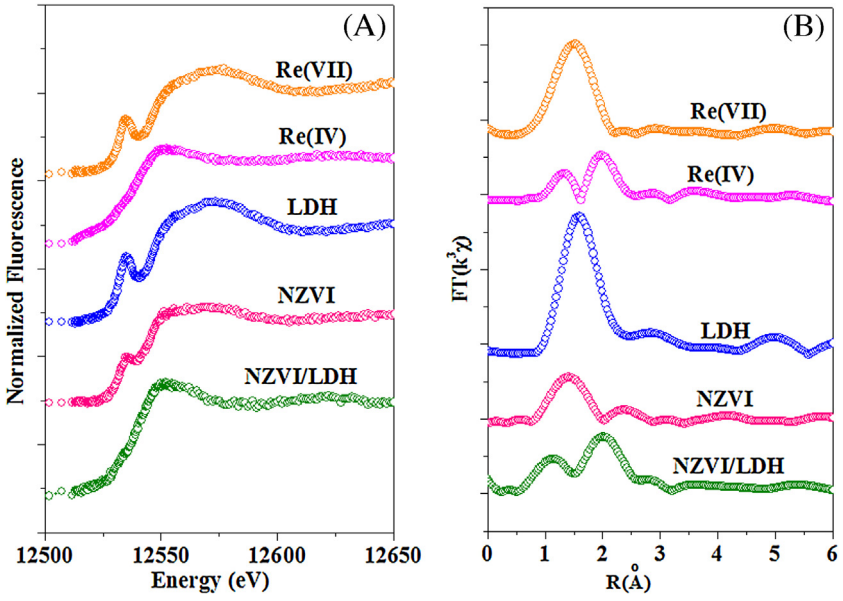

Fig. 5. (A) X-ray absorption near-edge structure (XANES), and (B) extended X-ray absorption fine structure (EXAFS) spectra of reference samples and reacted samples of Re(VII) immobilized onto LDH, NZVI and NZVI/LDH, respectively.

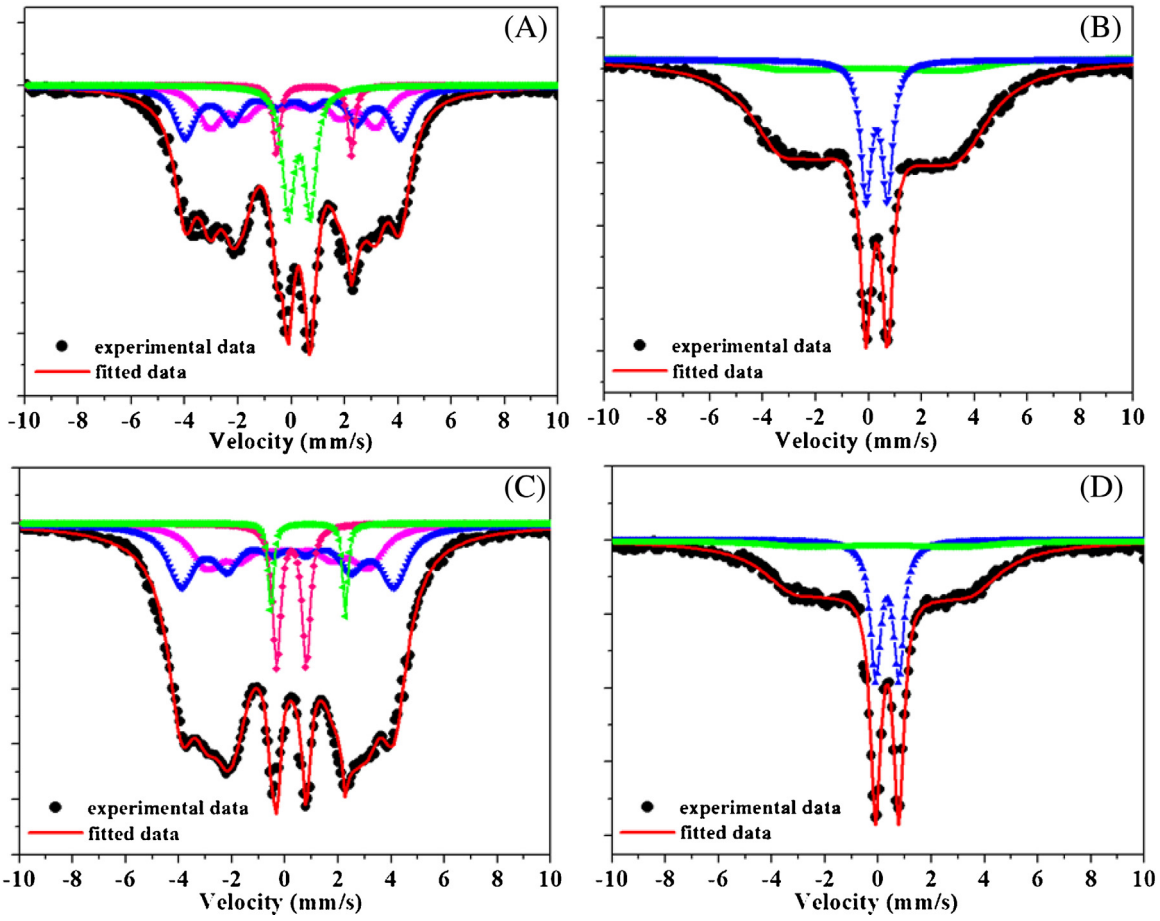

Fig. 6. ^{57}Fe Mössbauer spectra for the samples of NZVI and NZVI/LDH before and after reaction with Re(VII) from aqueous solutions. The points correspond to the experimental data and the continuous lines to the components used to fit the spectra.

tem than that in NZVI/LDH system. Namely, the efficiency of Re(VII) removal were 48.02% without coexisting anions in NZVI system, and 30.48% for SO_4^{2-}, 33.81% for $NaHCO_3^-$, 32.14% for Cl^-, 33.09% for PO_4^{3-}, respectively, while the efficiency were 91.16% without coexisting anions in NZVI/LDH system, and 80.25% for SO_4^{2-}, 82.15% for $NaHCO_3^-$, 79.54% for Cl^-, 80.97% for PO_4^{3-}, respectively. It was reported that LDH had strong sorption to coexisting anions via an ion exchange process [58]. The sorption of anions on LDH is believed to prevent formation of precipitates on NZVI/LDH, hence, more reactive sites can be used for Re(VII) reduction. This finding implies that LDH can act as a scavenger for coexisting anions, and thus weakened their inhibition effect.

3.3. *Identification of reaction products by MBS and XAFS*

To reveal the molecular mechanism of LDH as a support in the enhanced immobilization of Re(VII) by NZVI, X-ray absorption fine structure (XAFS) and Mössbauer spectra (MBS) were used for the identification and quantification of the reaction products. XAFS technique is very useful to determine the oxidation state and coordination environment of target metal ions sequestered onto surfaces at a molecular level, and has been widely used in previous reports [78–84]. Herein, the oxidation state and local atomic structure of Re sequestered onto the reactive materials can be identified by analyzing the X-ray absorption near-edge structure (XANES) and the extended X-ray absorption fine structure (EXAFS) parts of the XAFS spectra. Hence, we collected Re L_1-edge XANES and EXAFS spectra from the reference compounds (i.e., ReO_4^- and ReO_2) and Re(VII)-reacted LDH, NZVI and NZVI/LDH samples, and the results are shown in Fig. 5. From the normalized Re L_1-edge XANES (Fig. 5A), we can see that ReO_4^- ion with a tetrahedral coordination of Re, lacking an inversion center, exhibits a strong pre-edge peak, whereas, the pre-edge peak has nearly totally disappeared in case of ReO_2 with an octahedral coordination of Re. This is in good accordance with a previous report [85]. Therefore, we can conclude that the absence of this feature is evidence of Re(VII) reduction to lower oxidation state Re(IV) compounds. As we can see from Fig. 5A, the XANES spectrum of the sample for Re(VII)-reacted LDH resembles that of reference Re(VII), which is indicative of a sorption process for Re(VII) sequestered onto LDH. However, the XANES spectrum of the sample for Re(VII)-reacted NZVI/LDH resembles that of reference Re(IV), which is suggestive of a complete reduction process for Re(VII) sequestered onto NZVI/LDH. Nevertheless, for the sample of Re(VII)-reacted NZVI, the presence of a small pre-edge peak in the XANES spectrum demonstrates that Re(VII) is partly reduced into Re(IV) under our experimental conditions. Namely, some Re(VII) may be sequestered onto NZVI via a sorption mechanism. It is well known that surface passivation is an important process in NZVI-induced reduction system [62,67,68]. Herein, during the reduction of Re(VII) by NZVI, The insulating nature of the iron oxides/hydroxide formed in-situ prevented electron transfer from deeper iron core, hence bringing the redox reaction to a halt. So, the residual Re(VII) was adsorbed on the surface iron corrosion products. These results show that LDH can promote the nearly complete reduction of Re(VII) into Re(IV) in the NZVI reaction system.

The EXAFS spectra also exhibits significant different mechanism for Re(VII) sequestered onto various reactive materials. EXAFS spec-

Table 1
Values of the hyperfine parameters from the best fits of ^{57}Fe Mössbauer spectra for the samples of NZVI and NZVI/LDH before and after reaction with Re(VII) from aqueous solutions.

Samples	Iron species	Relative content (%)	IS (mm/s)	Q_S (mm/s)	HW (mm/s)	H_i/T
NZVI	Fe°	44.6	0.06 ± 0.03	0.05 ± 0.04	0.54 ± 0.10	19.3 ± 0.02
before reaction	Fe°	45.4	0.09 ± 0.02	−0.06 ± 0.02	0.48 ± 0.07	25.0 ± 0.16
	Fe^{2+}	1.6	0.88 ± 0.02	2.80 ± 0.05	0.15 ± 0.07	
	Fe^{3+}	8.4	0.32 ± 0.01	0.82 ± 0.02	0.26 ± 0.03	
NZVI	Fe°	78.7	0.21 ± 0.12	−0.07 ± 0.19	1.38 ± 0.48	21.0 ± 0.48
after reaction	Fe^{3+}	21.3	0.36 ± 0.01	0.87 ± 0.02	0.23 ± 0.02	
NZVI/LDH	Fe°	43.2	0.02 ± 0.02	−0.01 ± 0.02	0.71 ± 0.12	18.4 ± 0.31
before reaction	Fe°	53.4	0.05 ± 0.01	−0.03 ± 0.02	0.62 ± 0.06	24.5 ± 0.14
	Fe^{2+}	0.6	0.87 ± 0.02	2.80 ± 0.04	0.11 ± 0.03	
	Fe^{3+}	2.8	0.20 ± 0.01	1.19 ± 0.02	0.18 ± 0.03	
NZVI/LDH	Fe°	88.6	0.14 ± 0.04	−0.09 ± 0.06	1.38 ± 0.15	21.2 ± 0.23
after reaction	Fe^{3+}	11.4	0.33 ± 0.01	0.81 ± 0.01	0.24 ± 0.02	

Where IS the isomer shift (relative to α-Fe at RT), Q_S is the quadrupole splitting, HW is the half width at half maximum, H_i is the hyperfine magnetic field, relative content is the relative spectral absorption area for each specie.

tra were used to determine the local atomic structure of Re in Re(VII)-reacted LDH, NZVI and NZVI/LDH samples, and the results are shown in Fig. 5B. For the reference Re(VII), we can see that the peak for Re-O interaction is located at ~1.4 Å, while, for the reference Re(IV), the peak located at ~1.4 Å is for Re-O interaction and the peak located at ~2.2 Å is for Re–Re interaction. For the sample of Re(VII)-reacted LDH, the EXAFS spectrum is similar to that of Re(VII), i.e., only a peak at ~1.4 Å appears, indicating a sorption process. Meanwhile, for the sample of Re(VII)-reacted NZVI/LDH, the EXAFS spectrum is similar to that of Re(IV), i.e., both the peaks at ~1.4 Å and ~2.2 Å appear, demonstrating a complete reduction process and the reaction product is ReO_2. Besides, for the sample of Re(VII)-reacted NZVI, although both the peaks at ~1.4 Å and ~2.2 Å can be observed, the intensity of the peak at ~1.4 Å is higher than that at ~2.2 Å, which might be due to a mixture of Re(VII) and Re(IV). Namely, Re(VII) sequestered onto NZVI is a combination of sorption and reduction. Moreover, the small peaks at >2.5 Å may be due to the interaction from further neighbor atom (like Al or Mg) with Re, which suggests that LDH could react as a scavenger for the insoluble products, and thus decrease the accumulation of the insoluble products on iron surface. In this way, more reactive sites can be used for interfacial reaction, resulting in the enhancement of Re(VII) immobilization.

The species of iron on the surface of NZVI and NZVI/LDH before and after reaction with Re(VII) was further investigated by ^{57}Fe Mössbauer spectra (Fig. 6), and the Mössbauer hyperfine parameters are listed in Table 1.We can see that all the Fe°, Fe^{2+}, Fe^{3+} were present in both NZVI and NZVI/LDH samples before reaction. However, after reaction, only Fe° and Fe^{3+} were present in NZVI and NZVI/LDH [86]. This result indicates that the surface bound Fe(II) can participate in Re(VII) reduction. Besides, the relative content of Fe° (96.8%) for NZVI/LDH before reaction is much higher than that (90.0%) for NZVI, indicating that NZVI/LDH exhibited a good anti-oxidation performance. Furthermore, after reaction, the relative content of Fe° for NZVI/LDH only decreased from 96.8% to 88.6%, while the relative content of Fe° for NZVI decreased from 90.0%% to 78.7%, which displays the enhanced stability of NZVI/LDH during reaction, and thus leads to the improved reactivity of NZVI/LDH on removing and immobilizing Re(VII) in water. In a word, since zero valent iron has the advantages of low-cost and environment-friend [87–90], the LDH-supported NZVI composite will have potential application in environmental remediation.

4. Conclusion

In conclusion, LDH was proven to be an effective dispersant and stabilizer for NZVI in which the aggregation of NZVI was reduced and thus its reactivity was enhanced. As a result, NZVI/LDH was superior to bare NZVI in immobilizing Re(VII) from an aqueous solution due to the good synergistic effect between adsorption and reduction. The EXAFS measurements indicated that after Re(VII) reduction, the products (i.e., Re(IV)) became closely associated with the solid phase. The XANES results showed that Re(VII) can be almost completely reduced into Re(IV) by NZVI/LDH. Besides, NZVI/LDH displayed a good anti-oxidation performance as disclosed by ^{57}Fe Mössbauer spectra. The primary role of LDH in the enhancement of Re(VII) sequestration was also assumed to act as a pH buffering agents as well as a good scavenger for corrosion products and coexisting anions that inhibits the potential reactivity, increasing the reactivity of NZVI. To our knowledge, since LDH is stable and low-cost clay, consequently, the ability of LDH to be surface modified by anion exchange can be harnessed to create surface properties desirable for improved sorption of various contaminants, and to synthesize corresponding supported NZVI for enhanced sequestration of targeted contaminants. Herein, NZVI/LDH could be a promising and efficient remediation material and have potential implications for TcO_4^- sequestration from groundwater.

Acknowledgements

Financial supports from the National Natural Science Foundation of China (21577093, 21207092), Natural Science Foundation of Zhejiang Province (LY15B070001) is greatly acknowledged. We sincerely thank Dr. Xiang-xian Ma (Key Laboratory of Petroleum Resources, Gansu Province, 730000, P.R. China) for the measurement and analysis of Mössbauer spectra. The authors also thank beamline BL14W1 (Shanghai Synchrotron Radiation Facility) for providing the beam time.

Appendix A. Supplementary data

Supplementary data associated with this article can be found, in the online version, at http://dx.doi.org/10.1016/j.apcatb.2016.04.001.

References

[1] B.P. Burton-pye, I. Radivojevic, D. McGregor, I.M. Mbomekalle, W.W. Lukens Jr., L.C. Francesconi, Photoreduction of ^{99}Tc pertechnetate by nanometer-sized metal oxides: new strategies for formation and sequestration of low-valent technetium, J. Am. Chem. Soc. 133 (2011) 18802–18815.
[2] D. Fan, R.P. Anitori, B.M. Tebo, P.G. Tratnyek, J.S.L. Pacheco, R.K. Kukkadapu, M.H. Engelhard, M.E. Bowden, L. Kovarik, B.W. Arey, Reductive sequestration

of pertechnetate ($^{99}TcO_4^-$) by nano zerovalent iron (nZVI) transformed by abiotic sulfide, Environ. Sci. Technol. 47 (2013) 5302–5310.
[3] D. Fan, R.P. Anitori, B.M. Tebo, P.G. Tratnyek, J.S.L. Pacheco, R.K. Kukkadapu, L. Kovarik, M.H. Engelhard, M.E. Bowden, Oxidative remobilization of technetium sequestered by sulfide-transformed nano zerovalent iron, Environ. Sci. Technol. 48 (2014) 7409–7417.
[4] T. Wu, H. Wang, Q. Zheng, Y. Zhao, J. Li, Effect of EDTA on the diffusion behavior of $^{99}TcO_4^-$ and ReO_4^- in GMZ bentonite, J. Radioanal. Nucl. Chem. 299 (2014) 2037–2041.
[5] J. Li, W. Dai, G. Xiao, H. Wang, Z. Zhang, T. Wu, Pertechnetate diffusion in GMZ bentonite, J. Radioanal. Nucl. Chem. 293 (2012) 763–767.
[6] Y. Chung, B. Lee, K. Choo, S. Choi, Removal of perrhenate anions in aqueous solutions using anion-exchange organic/inorganic hybrid nanoporous beads, J. Ind. Eng. Chem. 17 (2011) 114–119.
[7] J.O. Dickson, J.B. Harsh, W.W. Lukens, E.M. Pierce, Perrhenate incorporation into binary mixed sodalites: the role of anion size and implications for technetium-99 sequestration, Chem. Geol. 395 (2015) 138–143.
[8] Z. Lou, J. Wang, X. Jin, L. Wan, Y. Wang, H. Chen, W. Shan, Y. Xiong, Brown algae based new sorption material for fractional recovery of molybdenum and rhenium from wastewater, Chem. Eng. J. 273 (2015) 231–239.
[9] M.J. Wharton, B. Atkins, J.M. Charnock, F.R. Livens, R.A.D. Pattrick, D. Collison, An X-ray absorption spectroscopy study of the coprecipitation of Tc and Re with mackinawite (FeS), Appl. Geochem. 15 (2000) 347–354.
[10] H. Liu, T. Qian, D. Zhao, Reductive immobilization of perrhenate in soil and groundwater using starch-stabilized ZVI nanoparticles, Chin. Sci. Bull. 58 (2013) 275–281.
[11] J. Li, C. Chen, R. Zhang, X. Wang, Reductive immobilization of Re(VII) by graphene modified nanoscale zero-valent iron particles using a plasma technique, Sci. China Chem. (2015), http://dx.doi.org/10.1007/s11426-015-5452-4.
[12] T. Peretyazhko, J.M. Zachara, S.M. Heald, R.K. Kukkadapu, C. Liu, A.E. Plymale, C.T. Resch, Reduction of Tc(VII) by Fe(II) sorbed on Al (hydr)oxides, Environ. Sci. Technol. 42 (2008) 5499–5506.
[13] D. Burghardt, E. Simon, K. Knöller, A. Kassahun, Immobilization of uranium and arsenic by ingestible iron and hydrogen stimulated autotrophic sulphate reduction, J. Contam. Hydrol. 94 (2007) 305–314.
[14] X. Guan, Y. Sun, H. Qin, J. Li, I.M.C. Lo, D. He, H. Dong, The limitations of applying zero-valent iron technology in contaminants sequestration and the corresponding countermeasures: the development in zero-valent iron technology in the last two decades (1994–2014), Water Res. 75 (2015) 224–248.
[15] L. Liang, X. Guan, Z. Shi, J. Li, Y. Wu, P.G. Tratnyek, Coupled effects of aging and weak magnetic fields on sequestration of selenite by zero-valent iron, Environ. Sci. Technol. 48 (2014) 6326–6334.
[16] L. Liang, W. Yang, X. Guan, J. Li, Z. Xu, J. Wu, Y. Huang, X. Zhang, Kinetics and mechanisms of pH-dependent Se(IV) removal by zero valent iron, Water Res. 47 (2013) 5846–5855.
[17] L. Liang, W. Sun, X. Guan, Y. Huang, W. Choi, H. Bao, L. Li, Z. Jiang, Weak magnetic field significantly enhances selenite removal kinetics by zero valent iron, Water Res. 1 (2014) 371–380.
[18] L. Liang, X. Guan, Y. Huang, J. Ma, X. Sun, J. Qiao, G. Zhou, Efficient selenate removal by zero-valent iron in the presence of weak magnetic field, Sep. Purif. Technol. 156 (2015) 1064–1072.
[19] Y. Sun, X. Guan, J. Wang, X. Meng, C. Xu, G. Zhou, Effect of weak magnetic field on arsenate and arsenite removal from water by zerovalent iron: an XAFS investigation, Environ. Sci. Technol. 48 (2014) 6850–6858.
[20] J. Li, Z. Shi, B. Ma, P. Zhang, X. Jiang, Z. Xiao, X. Guan, Improving the reactivity of zerovalent iron by taking advantage of its magnetic memory: implications for arsenite removal, Environ. Sci. Technol. 49 (2015) 10581–10588.
[21] L. Ling, W. Zhang, Enrichment and encapsulation of uranium with iron nanoparticle, J. Am. Chem. Soc. 137 (2015) 2788–2791.
[22] Q. Huang, X. Shi, R.A. Pinto, E.J. Petersen, W.J. Weber Jr., Tunable synthesis and immobilization of zero-valent iron nanoparticles for environmental applications, Environ. Sci. Technol. 42 (2008) 8884–8889.
[23] H. Paar, A.S. Ruhl, M. Jekel, Influences of nanoscale zero valent iron loadings and bicarbonate and calcium concentrations on hydrogen evolution in anaerobic column experiments, Water Res. 68 (2015) 731–739.
[24] X. Lv, Y. Hu, J. Tang, T. Sheng, G. Jiang, X. Xu, Effects of co-existing ions and natural organic matter on removal of chromium(VI) from aqueous solution by nanoscale zero valent iron (nZVI)-Fe_3O_4 nanocomposites, Chem. Eng. J. 218 (2013) 55–64.
[25] S.R. Kanel, J.M. Greneche, H. Choi, Arsenic(V) removal from groundwater using nano scale zero-valent iron as a colloidal reactive barrier material, Environ. Sci. Technol. 40 (2006) 2045–2050.
[26] O. Celebi, C. Üzüm, T. Shahwan, H.N. Erten, A radiotracer study of the adsorption behavior of aqueous Ba^{2+} ions on nanoparticles of zero-valent iron, J. Hazard. Mater. 148 (2007) 761–767.
[27] C. Ding, W. Cheng, Y. Sun, X. Wang, Effects of *Bacillus subtilis* on the reduction of U(VI) by nano-fe°, Geochim. Cosmochim. Acta 165 (2015) 86–107.
[28] Y. Xie, D.M. Cwiertny, Use of dithionite to extend the reactive lifetime of nanoscale zero-valent iron treatment systems, Environ. Sci. Technol. 44 (2010) 8649–8655.
[29] S. Bae, W. Lee, Influence of riboflavin on nanoscale zero-valent iron reactivity during the degradation of carbon tetrachloride, Environ. Sci. Technol. 48 (2014) 2368–2376.
[30] T. Phenrat, N. Saleh, K. Sirk, R.D. Tilton, G.V. Lowry, Aggregation and sedimentation of aqueous nanoscale zerovalent iron dispersions, Environ. Sci. Technol. 41 (2007) 284–290.
[31] C.M.D. Kocur, L. Lomheim, H.K. Boparai, A.I.A. Chowdhury, K.P. Weber, L.M. Austrins, E.A. Edwards, B.E. Sleep, D.M. O'Carroll, Contributions of abiotic and biotic dechlorination following carboxymethyl cellulose stabilized nanoscale zero valent iron injection, Environ. Sci. Technol. 49 (2015) 8648–8656.
[32] Y.H. Lin, H.H. Tseng, M.Y. Wey, M.D. Lin, Characteristics of two types of stabilized nano zero-valent iron and transport in porous media, Sci. Total Environ. 408 (2010) 2260–2267.
[33] F. He, D. Zhao, Preparation and characterization of a new class of starch-stabilized bimetallic nanoparticles for degradation of chlorinated hydrocarbons in water, Environ. Sci. Technol. 39 (2005) 3314–3320.
[34] F. He, M. Zhang, T. Qian, D. Zhao, Transport of carboxymethyl cellulose stabilized iron nanoparticles in porous media: column experiments and modeling, J. Colloid Interface Sci. 334 (2009) 96–102.
[35] I.C. Popescu, P. Filip, D. Humelnicu, I. Humelnicu, T.B. Scott, R.A. Crane, Removal of uranium(VI) from aqueous systems by nanoscale zero-valent iron particles suspended in carboxy-methyl cellulose, J. Nucl. Mater. 443 (2013) 250–255.
[36] S.M. Ponder, J.G. Darab, J. Bucher, D. Caulder, I. Craig, L. Davis, N. Edelstein, W. Lukens, H. Nitsche, L. Rao, D.K. Shuh, T.E. Mallouk, Surface chemistry and electrochemistry of supported zerovalent iron nanoparticles in the remediation of aqueous metal contaminants, Chem. Mater. 13 (2001) 479–486.
[37] J.G. Darab, A.B. Amonette, D.S.D. Burke, R.D. Orr, S.M. Ponder, B. Schrick, T.E. Mallouk, W.W. Lukens, D.L. Caulder, D.K. Shuh, Removal of pertechnetate from simulated nuclear waste streams using supported zerovalent iron, Chem. Mater. 19 (2007) 5703–5713.
[38] I. Dror, O.M. Jacov, A. Cortis, B. Berkowitz, Catalytic transformation of persistent contaminants using a new composite material based on nanosized zero-valent iron, ACS Appl. Mater. Interfaces 4 (2012) 3416–3423.
[39] Z. Chen, T. Wang, X. Jin, Z. Chen, M. Megharaj, R. Naidu, Multifunctional kaolinite-supported nanoscale zero-valent iron used for the adsorption and degradation of crystal violet in aqueous solution, J. Colloid Interface Sci. 398 (2013) 59–66.
[40] S. Luo, P. Qin, J. Shao, L. Peng, Q. Zeng, J. Gu, Synthesis of reactive nanoscale zero valent iron using rectorite supports and its application for orange II removal, Chem. Eng. J. 223 (2013) 1–7.
[41] G. Sheng, X. Shao, Y. Li, J. Li, H. Dong, W. Cheng, X. Gao, Y. Huang, Enhanced removal of U(VI) by nanoscale zerovalent iron supported on Na-bentonite and an investigation of mechanism, J. Phys. Chem. A 118 (2014) 2952–2958.
[42] C. Gu, H. Jia, H. Li, J.B. Teppen, A.S. Boyd, Synthesis of highly reactive subnanosized zero-valent iron using smectite clay templates, Environ. Sci. Technol. 11 (2010) 4258–4263.
[43] H. Jia, C. Gu, S.A. Boyd, B.J. Teppen, C.T. Johnston, C. Song, H. Li, Comparison of reactivity of nano-scaled zero-valent iron formed on clay surfaces, Soil Sci. Soc. Am. J. 75 (2010) 357–364.
[44] H. Jia, C. Wang, Adsorption and dechlorination of 2,4-dichlorophenol (2,4-DCP) on a multi-functional organo-smectite templated zero-valent iron composite, Chem. Eng. J. 191 (2012) 202–209.
[45] O.S. Arvaniti, Y. Hwang, H.R. Andersen, A.S. Stasinakis, N.S. Thomaidis, M. Aloupi, Reductive degradation of perfluorinated compounds in water using Mg-aminoclay coated nanoscale zero valent iron, Chem. Eng. J. 262 (2015) 133–139.
[46] Y. Hwang, Y. Lee, P.D. Mines, Y.S. Huh, H.R. Andersen, Nanoscale zero-valent iron (nZVI) synthesis in a Mg-aminoclay solution exhibits increased stability and reactivity for reductive decontamination, Appl. Catal. B: Environ. 147 (2014) 748–755.
[47] Y. Hwang, Y. Lee, P.D. Mines, Y. Oh, J.S. Choi, H.R. Andersen, Investigation of washing and storage strategy on aging of Mg-aminoclay (MgAC) coated nanoscale zero-valent iron (nZVI) particles, Chem. Eng. Sci. 119 (2014) 310–317.
[48] T. Zheng, J. Zhan, J. He, C. Day, Y. Lu, G.L. McPerson, G. Piringer, V.T. John, Reactivity characteristics of nanoscale zerovalent iron-silica composites for trichloroethylene remediation, Environ. Sci. Technol. 42 (2008) 4494–4499.
[49] M. Liu, Y. Wang, L. Chen, Y. Zhang, Z. Lin, $Mg(OH)_2$ supported nanoscale zero valent iron enhancing the removal of Pb(II) from aqueous solution, ACS Appl. Mater. Interfaces 7 (2015) 7961–7969.
[50] X. Lv, J. Xu, G. Jiang, X. Xu, Removal of chromium(VI) from wastewater by nanoscale zero-valent iron particles supported on multiwalled carbon nanotubes, Chemosphere 85 (2011) 1204–1209.
[51] G. Sheng, A. Alsaedi, W. Shammakh, S. Monaquel, J. Sheng, X. Wang, H. Li, Y. Huang, Enhanced sequestration of selenite in water by nanoscale zero valent iron immobilization on carbon nanotubes by a combined batch, XPS and XAFS investigation, Carbon 99 (2016) 123–130.
[52] J. Li, C. Chen, R. Zhang, X. Wang, Nanoscale zero-valent iron particles supported on reduced graphene oxides by using a plasma technique and their application for removal of heavy-metal ions, Chem. Asian J. 10 (2015) 1410–1417.
[53] Y. Sun, C. Ding, W. Cheng, X. Wang, Simultaneous adsorption and reduction of U(VI) on reduced graphene oxide-supported nanoscale zerovalent iron, J. Hazard. Mater. 280 (2014) 399–408.
[54] Z. Li, L. Wang, L. Yuan, C. Xiao, L. Mei, L. Zheng, J. Zhang, J. Yang, Y. Zhao, Z. Zhu, Z. Chai, W. Shi, Efficient removal of uranium from aqueous solution by

zero-valent iron nanoparticle and its grapheme composite, J. Hazard. Mater. 290 (2015) 26–33.
[55] W. Wang, Y. Cheng, T. Kong, G. Cheng, Iron nanoparticles decoration onto three-dimensional grapheme for rapid and efficient degradation of azo dye, J. Hazard. Mater. 299 (2015) 50–58.
[56] X. Lv, Z. Chen, Y. Wang, F. Huang, Z. Lin, Use of high-pressure CO_2 for concentrating Cr^{VI} from electroplating wastewater by Mg–Al layered double hydroxide, ACS Appl. Mater. Interfaces 5 (2013) 11271–11275.
[57] D. Zhao, G. Sheng, J. Hu, C. Chen, X. Wang, The adsorption of Pb(II) on Mg_2Al layered double hydroxide, Chem. Eng. J. 171 (2011) 167–174.
[58] K.H. Goh, T.T. Lim, Z. Dong, Application of layered double hydroxides for removal of oxyanions: a review, Water Res. 42 (2008) 1343–1368.
[59] Q. Wang, D. O'Hare, Recent advances in the synthesis and application of layered double hydroxide (LDH) nanosheets, Chem. Rev. 112 (2012) 4124–4155.
[60] S. Frey, S. Guilmet, R. Egan III, A. Bennett, S. Soltau, R. Holz, Immobilization of the aminopeptidase from aeromonas proteolytica on Mg^{2+}/Al^{3+} layered double hydroxide particles, ACS Appl. Mater. Interfaces 2 (2010) 2828–2832.
[61] S. Paušová, J. Krýsa, J. Jirkovský, G. Mailhot, V. Prevot, Photocatalytic behavior of nanosized TiO_2 immobilized on layered double hydroxides by delamination restacking process, Environ. Sci. Pollut. Res. 19 (2012) 3709–3718.
[62] G. Sheng, J. Hu, H. Li, J. Li, Y. Huang, Enhanced sequestration of Cr(VI) by nanoscale zero-valent iron supported on layered double hydroxide by batch and XAFS study, Chemosphere 148 (2016) 227–232.
[63] Y. Gao, C. Chen, H. Chen, R. Zhang, X. Wang, Synthesis of a novel organic–inorganic hybrid of polyaniline/titanium phosphate for Re(VII) removal, Dalton Trans. 44 (2015) 8917–8925.
[64] M. Rivero-Huguet, W.D. Marshall, Reduction of hexavalent chromium mediated by micro- and nano-sized mixed metallic particles, J. Hazard. Mater. 169 (2009) 1081–1087.
[65] R. Cheng, J. Wang, W. Zhang, Comparison of reductive dechlorination of p-chlorophenol using Fe° and nanosized Fe°, J. Hazard. Mater. 144 (2007) 334–339.
[66] G.V. Lowry, K.M. Johnson, Congener-specific dechlorination of dissolved PCBs by microscale and nanoscale zerovalent iron in a water/methanol solution, Environ. Sci. Technol. 38 (2004) 5208–5216.
[67] Y. Li, J. Li, Y. Zhang, Mechanism insights into enhanced Cr(VI) removal using nanoscale zerovalent iron supported on the pillared bentonite by macroscopic and spectroscopic studies, J. Hazard. Mater. 227 (2012) 211–218.
[68] Y. Li, W. Cheng, G. Sheng, J. Li, H. Dong, Y. Chen, L. Zhu, Synergetic effect of a pillared bentonite support on Se(VI) removal by nanoscale zero valent iron, Appl. Catal. B: Environ. 174–175 (2015) 329–335.
[69] Y. Oh, H. Song, W. Shin, S. Choi, Y. Kim, Effect of amorphous silica and silica sand on removal of chromium(VI) by zero-valent iron, Chemosphere 66 (2007) 858–865.
[70] D.W. Cho, C.M. Chon, B.H. Jeon, Y. Kim, M.A. Khan, H. Song, The role of clay minerals in the reduction of nitrate in groundwater by zero-valent iron, Chemosphere 81 (2010) 611–616.
[71] Y. Mu, Z. Ai, L. Zhang, F. Song, Insight into core–shell dependent anoxic Cr(VI) removal with $Fe@Fe_2O_3$ nanowires: indispensable role of surface bound Fe(II), ACS Appl. Mater. Interfaces 7 (2015) 1997–2005.
[72] S. Yan, Y. Chen, W. Xiang, Z. Bao, C. Liu, B. Deng, Uranium(VI) reduction by nanoscale zero-valent iron in anoxic batch systems: the role of Fe(II) and Fe(III), Chemosphere 117 (2014) 625–630.
[73] T. Peretyazhko, J.M. Zachara, S.M. Heald, B.H. Jeon, R.K. Kukkadapu, C. Liu, D.A. Moore, C.T. Resch, Heterogeneous reduction of Tc(VII) by Fe(II) at the solid-water interface, Geochim. Cosmochim. Acta 72 (2008) 1521–1539.
[74] D.P. Jaisi, H. Dong, A.E. Plymale, J.K. Fredrickson, J.M. Zachara, S. Heald, C. Liu, Reduction and long-term immobilization of technetium by Fe(II) associated with clay mineral nontronite, Chem. Geol. 264 (2009) 127–138.
[75] H.S. Kim, J.Y. Ahn, C. Kim, S. Lee, I. Hwang, Effect of anions and humic acid on the performance of nanoscale zero-valent iron particles coated with polyacrylic acid, Chemosphere 113 (2014) 93–100.
[76] J. Chen, Z. Xiu, G.V. Lowry, P.J.J. Alvarez, Effect of natural organic matter on toxicity and reactivity of nano-scale zero-valent iron, Water Res. 45 (2011) 1995–2001.
[77] J. Klausen, P.J. Vikesland, T. Kohn, D.R. Burris, W.P. Ball, A.L. Roberts, Longevity of granular iron in groundwater treatment processes: solution composition effects on reduction of organohalides and nitroaromatic compounds, Environ. Sci. Technol. 37 (2003) 1208–1218.
[78] G. Sheng, S. Yang, Y. Li, X. Gao, Y. Huang, X. Wang, Retention mechanisms and microstructure of Eu(III) on manganese dioxide studied by batch and high resolution EXAFS technique, Radiochim. Acta 102 (2014) 155–167.
[79] G. Sheng, L. Ye, Y. Li, H. Dong, H. Li, X. Gao, Y. Huang, EXAFS study of the interfacial interaction of nickel(II) on titanate nanotubes: role of contact time pH and humic substances, Chem. Eng. J. 248 (2014) 71–78.
[80] G. Sheng, S. Yang, D. Zhao, J. Sheng, X. Wang, Adsorption of Eu(III) on titanate nanotubes studied by a combination of batch and EXAFS technique, Sci. China: Chem. 55 (2012) 182–194.
[81] G. Sheng, H. Dong, R. Shen, Y. Li, Microscopic insights into the temperature-dependent adsorption of Eu(III) onto titanate nanotubes studied by FTIR, XPS XAFS and batch technique, Chem. Eng. J. 217 (2013) 486–494.
[82] G. Sheng, Q. Yang, F. Peng, H. Li, X. Gao, Y. Huang, Determination of colloidal pyrolusite, Eu(III) and humic substance interaction: a combined batch and EXAFS approach, Chem. Eng. J. 245 (2014) 10–16.
[83] G. Sheng, S. Yang, J. Sheng, J. Hu, X. Tan, X. Wang, Macroscopic and microscopic inve stigation of Ni(II) sequestration on diatomite by batch XPS and EXAFS techniques, Environ. Sci. Technol. 45 (2011) 7718–7726.
[84] G. Sheng, R. Shen, H. Dong, Y. Li, Colloidal diatomite, radionickel and humic substance interaction: a combined batch XPS and EXAFS investigation, Environ. Sci. Poll. Res. 20 (2013) 3708–3717.
[85] M. Fröba, K. Lochte, W. Metz, XANES studies on rhenium L absorption edges of Re_2O_7 graphite intercalation compounds and of other rhenium-oxygen compounds, J. Phys. Chem. Solids 57 (1996) 635–641.
[86] E. Petala, K. Dimos, A. Douvalis, T. Bakas, J. Tucek, R. Zboril, M.A. Karakassides, Nanoscale zero-valent iron supported on mesoporous silica: characterization and reactivity for Cr(VI) removal from aqueous solution, J. Hazard. Mater. 261 (2013) 295–306.
[87] Y.H. Huang, C. Tang, H. Zeng, Removing molybdate from water using a hybridized zero-valent iron/magnetite/Fe(II) treatment system, Chem. Eng. J. 200–202 (2012) 257–263.
[88] C. Tang, Y.H. Huang, H. Zeng, Z. Zhang, Reductive removal of selenate by zero-valent iron: the roles of aqueous Fe^{2+} and corrosion products, and selenate removal mechanisms, Water Res. 67 (2014) 166–274.
[89] C. Tang, Y. Huang, Z. Zhang, J. Chen, H. Zeng, Y.H. Huang, Rapid removal of selenate in a zero-valent iron/Fe_3O_4/Fe^{2+} synergetic system, Appl. Catal. B: Environ. 184 (2016) 320–327.
[90] J. Li, H. Qin, X. Guan, Premagnetization for enhancing the reactivity of multiple zerovalent iron samples toward various contaminants, Environ. Sci. Technol. 49 (2015) 14401–14408.